Original Article

Intraretinal Segmentation on Fourier Domain Optical Coherence Tomography

Jingjing Huang,[1] MD, PhD, Xing Liu,[1] MD, PhD, Ziqiang Wu,[2] MD, Dan Cao,[1] MD, Srinivas Sadda,[3] MD

Abstract

Introduction: We studied the automated intraretinal segmentation on Fourier domain optical coherence tomography (OCT). Materials and Methods: Thirty eyes from 30 normal subjects were studied using the RTVue-100. Both radial and raster scan protocol were performed 3 times on each subject. The OCT software performs automated intraretinal segmentation and provides macular thickness measurements. Results: Both scanning protocols provide reproducible inner, outer and full retinal thickness measurements. The inner, outer and full retinal thicknesses at the foveal central subfield were 67.31 ± 12.27 μm, 151.67 ± 12.96 μm, 219.33 ± 23.19 μm, respectively by the raster scan, and 63.27 ± 10.37 μm, 147.07 ± 14.54 μm, 209.89 ± 21.80 μm, respectively by the radial scan. Macular regional variations were consistently observed. The raster scan protocol gives greater retinal thickness measurements than the radial scan protocol (P <0.05), but the latter yields slightly more reproducible results. Conclusions: Fourier domain OCT equipped with the ability to perform automatic intraretinal segmentation is a convenient tool in studying diseases that may differentially affect various parts of the retina. However, the establishment of normative values can be complicated by different scanning protocols, devices used, methods of data presentation and definition of intraretinal boundaries.

Ann Acad Med Singapore 2010;39:518-24

Key words: Histology, Image processing, Retina/anatomy

Introduction

Optical coherence tomography (OCT) has become an indispensable tool in the management of retinal and optic nerve diseases as well as in clinical trials.[1-5] In late 1996, the earliest commercially available OCT had an axial resolution of approximately 17 μm. Using either animal or human cadaver retinas, several investigators attempted to correlate histology with OCT images.[6,7] However, because of the limitation of resolution, it was found that although OCT bands may be partially correlated to specific retinal layers, it was only due to their individual and combined optical properties, many of which were poorly understood.[8] In addition, commercially available OCTs only allowed the delineation of a limited number of retinal sublayers.[8] By 2002, the axial resolution of the latest time-domain OCT (Stratus OCT, Carl Zeiss Meditec, Dublin, CA) had improved to about 10 μm, allowing different investigators to develop software algorithms to perform automated segmentation more precisely on the Stratus OCT.[9,10]

The emergence of ultrabroad bandwidth femtosecond laser technology[11] facilitated the development of ultra high resolution OCT (UHR OCT) with axial resolution of approximately 3 μm in the human retina. By comparing pig and primate histological sections and cross-sectional tomographic images, Gloesmann et al[12] and Anger et al[13] demonstrated that the UHR OCT can visualise various retinal layers which had thus far only been possible with histological sectioning. The use of UHR OCT is still largely confined to the laboratory, but advances in OCT technology known as Fourier domain (FD) or spectral domain (SD) have significantly improved the scanning speed and sensitivity of these devices. The axial resolution of most commercially available FD OCTs is 5~7 μm, which makes retinal segmentation and interpretation more accurate and intuitive.

The RTVue-100 (Optovue, Fremont, CA) is an FD OCT which provides a software programme to automatically segment the retina into the inner and outer portions by delineating the boundary between the inner nuclear layer and the outer plexiform layer. Using the RTVue-100, Lim et

[1] State Key Laboratory of Ophthalmology, Zhongshan Ophthalmic Center, Sun Yat-sen University, Guangzhou, China
[2] Center for Advanced Eye Care, Carson City, Nevada, USA
[3] Doheny Image Reading Center, Doheny Eye Institute, Los Angeles, California, USA
Address for Correspondence: Dr Xing Liu, State Key Laboratory of Ophthalmology, Zhongshan Ophthalmic Center, Sun Yat-sen University, 54 Xianlienan Road, Guangzhou 510060, China.
Email: drliuxing@163.com

al[14] found a significant decrease in the inner retinal thickness of patients with retinal dystrophy compared to normal subjects. However, there are at present, very few published reports on the normative values of the inner and outer retinal thicknesses. In the current study, we performed 2 macular scanning protocols available in the RTVue-100 in normal subjects with the goal of establishing normative values and comparing the results of these 2 different scanning protocols on the automated intraretinal segmentation algorithm.

Materials and Methods

Patients

Normal subjects were recruited at the Zhongshan Ophthalmic Centre of Sun Yat-sen University, Guangzhou, China, between February and July 2008. The study was conducted in accordance with the tenets of the Declaration of Helsinki and was approved by the Institutional Review Board. Informed consent were obtained from all subjects.

All subjects underwent complete ophthalmic evaluation including best-refracted visual acuity, applanation tonometry, slit-lamp biomicroscopy, dilated stereoscopic examination, fundus photography, and Humphrey SITA standard 24-2 or 30-2 visual field testing.

The inclusion criteria were: (i) aged between 20 and 60 years old, (ii) best refracted Snellen visual acuity 20/20 or better, (iii) refractive error not exceeding 3 diopters spherical equivalent (hyperopia or myopia) and 1 diopter cylinder, (iv) intraocular pressure <21 mmHg by Goldmann applanation tonometry, (v) normal optic nerve and macula appearance by dilated stereoscopic examination and fundus photography, (vi) normal visual field by Humphrey perimetry, (vii) no medical or family history of retinal disease or glaucoma, (viii) no medical or family history of diabetes mellitus and (ix) no prior ocular surgery.

Optical Coherence Tomography

For each consecutive, eligible subject, one eye was randomly chosen to be scanned following pharmacological pupillary dilation. Two different protocols of the RTVue-100 (version 2.6), the mm6 and the mm5, were used (Fig. 1). The mm6 protocol performs 12 radial line scans consisting of 1024 A-scans each (6 mm scan length) centered on the fovea. The total scan time is 0.27 seconds. The mm5 protocol performs raster scans which include 11 horizontal and 11 vertical scans in 0.5 mm intervals. Each line scan consists of 668 A-scans over a 5 mm scan length. Additionally, the mm5 protocol also performs 6 horizontal and 6 vertical scanning lines in 0.5 mm intervals. Each of these scans consists of 400 A-scans over a 3 mm scan length. The total scanning time is about 0.78 seconds. For both protocols, the analysis software performs data interpolation for the unscanned areas and then reconstructs a false-colour topographic image displayed with numeric averages of the thickness measurements for each of the 9 map sectors as defined by the Early Treatment of Diabetic Retinopathy Study[15] (ETDRS) (Fig. 2). Unlike the foveal central subfield (FCS), the middle and outer rings are each divided into 4 quadrants (superior, inferior, nasal, temporal). The middle ring has a diameter of 3 mm for both protocols. However, the mm6 and mm5 define retinal thicknesses in the outer ring differently due to different scan areas. In the mm5 protocol, which has a square scan area, the outer ring displays the average thicknesses of the retinal areas located between 3 to 5 mm from the foveal centre. The mm6 protocol has a circular scan area, so the outer ring simply displays the average retinal thicknesses between the 3 mm and 6 mm rings. FCS thickness was defined as the average thickness in the inner 1 mm diameter circle (C1) of the ETDRS grid. For ease of discussion, the superior subfield in the middle ring for both protocols was labelled S3, while the nasal subfield in the 5 mm (mm5 protocol) and 6 mm (mm6 protocol) outer rings were respectively labelled N5 and N6, etc. (Fig. 2). The RTVue-100 software also calculates the macular volume within the scanned areas (within the 1 mm circle, the middle 3 mm ring, and the outer 5 or 6 mm rings).

The analysis software of both the mm6 and the mm5 protocols automatically divides the inner and outer neurosensory retinas at the boundary between the inner nuclear layer and the outer plexiform layer (Fig. 3). The thicknesses of the full retina as well as the inner and outer retinal layers are displayed topographically in each of the ETDRS map sectors.

OCT imaging was performed 3 times on each subject using both scan protocols in one visit by the same physician examiner (JH). Each scan was carefully reviewed to make sure that the automatic boundary detection was performed correctly. Scans were repeated if they were found to be de-centered or were determined to have segmentation errors. Such suboptimal scans were excluded from analysis. Individual measurements from the 3 scans were averaged for each ETDRS macular subfield parameter and used for comparisons. The mean, the standard deviation, the coefficient of variation (CV = standard deviation divided by mean) and the intraclass correlation coefficient (ICC) for each parameter were calculated.

Statistical Analysis

One way ANOVA was used to compare retinal thicknesses among different ETDRS regions and to compare the CVs among full (FRL), inner (IRL) and outer (ORL) retinal layer measurements. Where appropriate, the ETDRS subfield measurements of IRL, ORL and FRL by the mm6 protocol were compared with the corresponding results from the mm5 protocol using paired *t*-tests.

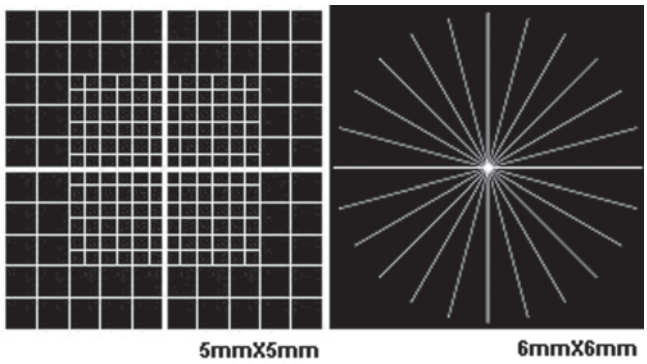

Fig. 1. Scanning pattern and retinal thickness maps produced by of the mm5 (left panel) and mm6 (right panel) protocols of the RTVue-100 Fourier domain optical coherence tomography instrument.

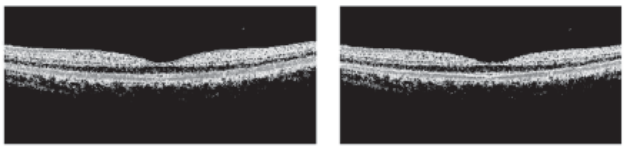

Fig. 3. The retinal segmentation of the inner and outer retina by the automated programme of the RTVue-100 OCT.

To assess the effect size of the differences in macular measurements between the mm5 and mm6 scanning protocols, the effect size θ was calculated as

$$\theta = \frac{\mu_1 - \mu_1}{\sigma}$$

where μ_1 and μ_2 were the mean macular thickness measurements by the mm5 and mm6 protocol, respectively and σ was the standard deviation of the mm6 measurement.

Results

Thirty eyes (15 left eyes, 15 right eyes) from 30 normal subjects (all Chinese) were examined clinically and by the RTVue-100. The average age was 42.67 ± 9.68 years (range, 21 to 55). There were 19 men and 11 women.

Both scanning protocols showed that the IRL, ORL and FRL were thinnest in the FCS, thickest in the middle ring, then gradually thinned toward the outer ring (Table 1, Fig. 4). In the FCS, IRL accounted for 30% of FRL thickness, versus about 43% in the middle and outer rings.

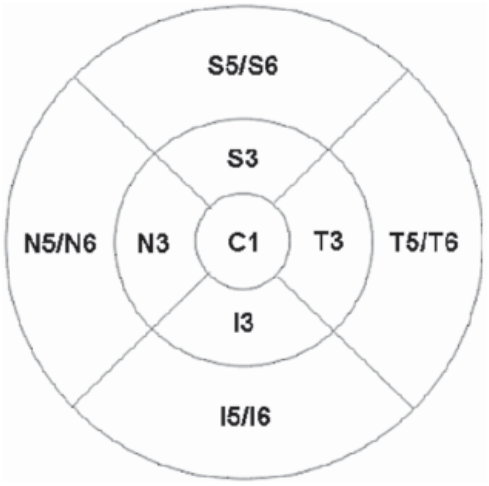

Fig. 2. The early treatment of Diabetic Retinopathy Study (ETDRS) macular map sectors.

Outer ring thicknesses (5/6 mm diameter for mm5/mm6)

There were significant differences in the FRL, IRL, and ORL thickness measurements between the mm6 and mm5 protocols. The mm5 protocol yielded about 10 μm greater FRL thicknesses, 5 μm greater IRL thicknesses, and 4 μm greater ORL thicknesses in the FCS and the middle ring than the mm6 protocol, but the effect sizes of the differences were comparable within each retinal segmentation subgroup (Table 1). Because the measured areas were different, comparisons of the outer ring thicknesses were not made between the 2 protocols.

For most ETDRS map sector parameters investigated by the mm5 and mm6 protocols, the CVs of the FRL measurements were less than those of the ORL, which in turn were less than those of the IRL (Table 2). The ICCs of the FRL measurements were greater than those of the ORL, which in turn were greater than those of the IRL (Table 3). However, there were generally no statistically significant differences in CVs between the 2 scanning protocols (Table 2).

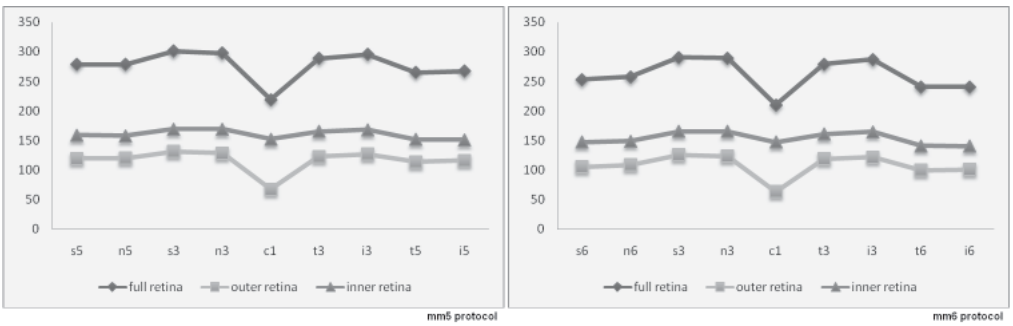

Fig. 4. The full, inner and outer retinal thicknesses measured by the mm5 and the mm6 scanning protocols.

Table 1. The Full, Inner and Outer Retinal Thicknesses in ETDRS Map Sectors Measured by the mm6 and the mm5 Protocols of the RTVue-100 (Retinal Thicknesses in μm, Retinal Volumes in mm^3)

		Full retina				Inner retina				Outer retina			
Region		**mm5**	**mm6**	**Effect size**	***P***	**mm5**	**mm6**	**Effect size**	***P***	**mm5**	**mm6**	**Effect size**	***P***
Foveal central subfield thickness (1 mm diameter, C1)		219.33 ±23.19	209.89 ±21.80	0.433	0.000	67.31 ±12.27	63.27 ±10.37	0.390	0.000	151.67 ±12.96	147.07 ±14.54	0.316	0.000
Middle ring thicknesses (3 mm diameter)	Superior (S3)	301.22 ±22.83	290.39 ±23.08	0.469	0.000	131.20 ±12.58	125.53 ±13.20	0.430	0.000	169.33 ±14.63	165.31 ±14.49	0.277	0.004
	Nasal (N3)	298.01 ±22.51	288.74 ±22.84	0.406	0.000	128.44 ±12.89	123.82 ±13.04	0.354	0.000	168.88 ±13.91	165.44 ±14.99	0.229	0.024
	Inferior (I3)	295.97 ±20.97	286.54 ±19.76	0.477	0.000	127.18 ±10.81	121.93 ±10.52	0.499	0.001	168.07 ±15.51	164.89 ±14.70	0.216	0.017
	Temporal (T3)	288.70 ±22.61	278.89 ±20.33	0.483	0.000	123.04 ±11.37	118.77 ±10.46	0.408	0.000	165.17 ±14.44	160.47 ±13.99	0.336	0.000
Outer ring thicknesses (5/6 mm diameter for mm5/mm6)	Superior (S5/6)	278.49 ±15.66	252.82 ±14.85	/	/	119.48 ±5.96	105.67 ±5.81	/	/	158.57 ±12.18	147.44 ±11.56	/	/
	Nasal (N5/6)	278.23 ±19.82	257.19 ±18.49	/	/	120.19 ±8.12	108.99 ±7.87	/	/	157.73 ±14.73	148.89 ±13.61	/	/
	Inferior (I5/6)	267.53 ±18.75	240.14 ±17.00	/	/	116.10 ±8.29	100.50 ±8.60	/	/	150.96 ±11.56	140.14 ±11.17	/	/
	Temporal (T5/6)	265.26 ±15.66	240.52 ±13.14	/	/	113.64 ±6.05	100.00 ±6.66	/	/	151.42 ±11.05	141.11 ±10.90	/	/
Volume	1 mm	0.172 ±0.018	0.165 ±0.017	0.412	0.000	0.053 ±0.010	0.050 ±0.008	0.375	0.000	0.119 ±0.010	0.116 ±0.011	0.273	0.000
	3 mm	2.032 ±0.150	1.963 ±0.144	0.479	0.000	0.853 ±0.078	0.819 ±0.074	0.459	0.000	1.174 ±0.095	1.146 ±0.095	0.295	0.001
	5/6 mm	5.461 ±0.325	7.215 ±0.409	/	/	2.327 ±0.142	3.021 ±0.187	/	/	3.116 ±0.225	4.275 ±0.437	/	/

Discussion

Many researchers have found that different diseases may cause changes in specific intraretinal layers,[16-20] while pathology in various intraretinal layers may respond differently to treatments.[21] Therefore, studying and quantifying only the whole retina, without considering the various parts, may neglect potentially valuable insights into disease pathophysiology.

Software algorithm designed to take advantage of different reflectivities of various layers can be utilised to study intraretinal pathology.[12,13,22-25] While tremendously helpful, these protocols still require validation and establishment of normative databases. There have been few studies investigating the thicknesses of IRL, ORL and FRL in normal subjects, and even fewer using FD OCT technology. Complicating matters further is the fact that different FD OCTs have slightly different segmentation algorithms for the outer boundary of the retina, which are also different compared to earlier generations of OCT.[26] Therefore, normative values need to be established for each device.

Using the Stratus OCT software and an additional image analysis programme developed in Matlab (Mathworks, Natick, Massachusetts, USA), Shahidi et al[10] performed segmentation measurement of the full, inner (which included the outer plexiform layer), and outer retinal layers on 10 normal subjects using the OCT3. Similar studies on normal subjects using FD OCT devices have thus far been very limited. In a study of 10 normal subjects using a software developed in Matlab based on a 2-dimensional automated edge detection scheme, Bagci et al[22] found that the computer segmentation algorithm of the RTVue-100 mm5 protocol gives thickness results of 6 retinal sublayers that are within 4 to 9 μm (root mean squared error) of manual measurements. While relatively small, this study provided evidence that

Table 2. The Coefficients of Variation of the Full, Inner and Outer Retinal Thickness Measurements by the mm6 and the mm5 Protocols on the ETDRS Map (Statistically Significant Differences in Bold)

		Full retina			Inner retina			Outer retina		
Region		**mm5**	**mm6**	***P***	**mm5**	**mm6**	***P***	**mm5**	**mm6**	***P***
Fovea Central Subfield Thickness (1 mm diameter, C1)		1.81	1.37	0.073	4.22	3.82	0.478	1.68	1.19	**0.013**
Middle ring thicknesses (3 mm diameter)	Superior (S3)	1.03	1.06	0.882	2.83	3.27	0.330	2.06	2.59	0.176
	Nasal (N3)	1.00	1.00	0.985	3.32	3.09	0.672	2.10	2.15	0.910
	Inferior (I3)	1.26	0.93	0.128	3.61	3.75	0.853	2.97	2.63	0.514
	Temporal (T3)	1.41	0.97	**0.046**	3.10	3.02	0.861	1.92	1.98	0.876
Volume	1 mm	0.85	0.56	0.195	3.96	3.74	0.700	1.64	1.13	**0.013**
	3 mm	0.90	0.70	0.201	2.55	2.54	0.987	1.65	1.79	0.649

Table 3. The Intraclass Correlation Coefficient of the 3 Repeated Measurements of the Full, Inner and Outer Retinal Thickness Measurements by the mm6 and the mm5 Protocols on the ETDRS Map

		Full retina		Inner retina		Outer retina	
Region		**mm5**	**mm6**	**mm5**	**mm6**	**mm5**	**mm6**
Fovea Central Subfield Thickness (1 mm diameter, C1)		0.962	0.973	0.942	0.928	0.957	0.978
Middle ring thicknesses (3 mm diameter)	Superior (S3)	0.967	0.968	0.897	0.865	0.929	0.884
	Nasal (N3)	0.973	0.974	0.817	0.859	0.895	0.902
	Inferior (I3)	0.946	0.973	0.757	0.701	0.868	0.866
	Temporal (T3)	0.950	0.971	0.872	0.828	0.923	0.905
Outer ring thicknesses (5/6 mm diameter)	Superior (S5/6)	0.950	0.962	0.842	0.864	0.923	0.951
	Nasal (N5/6)	0.973	0.987	0.823	0.890	0.933	0.954
	Inferior (I5/6)	0.931	0.974	0.763	0.932	0.926	0.903
	Temporal (T5/6)	0.922	0.942	0.738	0.952	0.949	0.958
Volume	1 mm	0.945	0.982	0.945	0.931	0.959	0.979
	3 mm	0.971	0.983	0.889	0.864	0.937	0.923
	5/6 mm	0.963	0.974	0.871	0.930	0.956	0.958

the RTVue-100's intraretinal segmentation algorithm was fairly accurate in normal eyes.

In the study by Lim et al,[14] comparing normal subjects with retinal dystrophy patients on the RTVue-100, the area-weighted macular thickness measurements averaged over the central 5 mm diameter region in normal subjects were 109.9 μm for IRL, 182.9 μm for ORL and 292.8 μm for FRL. Our measurements with the mm5 protocol were 118.59 μm for IRL, 158.93 μm for ORL and 277.82 μm for FRL. Even though both studies were done on the same device, several major differences may explain the disparate findings. In the study by Lim et al, the inner retinal layer was defined as the distance from the internal limiting membrane to the outer boundary of the inner plexiform layer because some retinal dystrophy patients did not have clearly demarcated outer plexiform layers on the OCT images. In our study, the automatic segmentation algorithm of the RTVue-100 included the inner nuclear layer as part of the IRL. The study by Lim et al utilised horizontal and vertical line scans, versus the mm5 protocol in our study. Finally, discrepancies in retinal thicknesses may also be partially due to different ethnicities of the subjects.

Another pitfall when comparing studies arises from the varying methods used to calculate average thicknesses. In most studies of intraretinal segmentation,[8,10,22] the average retinal thickness (IRL, ORL or FRL) is calculated as the average thickness along a cross-section of the retina, which should be the area of the scanned retina divided by the scan length. However, the ETDRS grid, which is sometimes a more convenient way of following retinal thickness changes

over time, would require area-weighted adjustments. On a radial scan, scan points farther away from the fovea are spaced further apart. Therefore, they represent a larger area of the retina and should be given greater weight. For each ETDRS subfield, the average thickness would be the retinal volume of the subfield divided by the area. These 2 different ways of computing average thickness cannot be easily compared.

In addition to providing normative values, our study demonstrates that various scanning protocols may yield different results on the RTVue-100. While the mm6 protocol covers a slightly larger area, the mm5 protocol has greater sampling density (Fig. 1). However, the results of these 2 protocols correlate with each other and have relatively low variability, given the low CV and high ICC of the 3 repeated measurements, consistent effect size of the difference between the 2 protocols, and the consistent macular regional variations. The higher sampling density of the mm5 would theoretically reduce variability, but the longer scan time required may have cancelled out this benefit.

Our study demonstrates that the mm5 protocol gives significantly higher retinal thickness measurements than the mm6 (Table 1). The former, because of its higher sampling density and a more even distribution of scan points, requires less data interpolation compared to the mm6. Additionally, the methods of data interpolation, which are not available from the manufacturer, may be slightly different. To our knowledge, a difference in retinal thickness measurements between the raster and the radial scans has not been demonstrated on other devices.

As illustrated by the existing literature and our study, comparing different studies and establishing normative values can be complicated by different scanning protocols, OCT devices used, methods of data presentation (cross-sectional retinal profile vs ETDRS grid) and demographic factors. Studying the segmentation of intraretinal layers is made more complex by different definitions of the boundary between the inner and outer retinas. Nevertheless, the data from this study may be useful for future investigation into diseases that have differential effects on various intraretinal structures.

Acknowledgements

This study was supported by Grant 30901648 from the National Natural Science Foundation of China.

REFERENCES

1. Hee MR, Izatt JA, Swanson EA, Huang D, Schuman JS, Lin CP, et al. Optical coherence tomography of the human retina. Arch Ophthalmol 1995;113:325-32.
2. Hee MR, Puliafito CA, Wong C, Duker JS, Reichel E, Rutledge B, et al. Quantitative assessment of macular edema with optical coherence tomography. Arch Ophthalmol 1995;113:1019-29.
3. Puliafito CA, Hee MR, Lin CP, Reichel E, Schuman JS, Duker JS, et al. Imaging of macular diseases with optical coherence tomography. Ophthalmology 1995;102:217-29.
4. Schuman JS, Hee MR, Puliafito CA, Wong C, Pedut-Kloizman T, Lin CP, et al. Quantification of nerve fiber layer thickness in normal and glaucomatous eyes using optical coherence tomography. Arch Ophthalmol 1995;113:586-96.
5. Liu X, Ling Y, Gao R, Zhao T, Huang J, Zheng X. Optical coherence tomography's diagnostic value in evaluating surgical impact on idiopathic macular hole. Chin Med J (Engl) 2003;116:444-7.
6. Huang Y, Cideciyan AV, Papastergiou GI, Banin E, Semple-Rowland SL, Milam AH, et al. Relation of optical coherence tomography to microanatomy in normal and rd chicken. Invest Ophthalmol Vis Sci 1998;39:2405-16.
7. Toth CA, Narayan DG, Boppart SA, Hee MR, Fujimoto JG, Birngruber R, et al. A comparison of retinal morphology viewed by optical coherence tomography and by light microscopy. Arch Ophthalmol 1997;115:1425-8.
8. Chauhan DS, Marshall J. The interpretation of optical coherence tomography images of the retina. Invest Ophthalmol Vis Sci 1999;40:2332-42.
9. Ishikawa H, Stein DM, Wollstein G, Beaton S, Fujimoto JG, Schuman JS. Macular segmentation with optical coherence tomography. *Invest Ophthalmol Vis Sci* 2005;46:2012-7.
10. Shahidi M, Wang Z, Zelkha R. Quantitative thickness measurement of retinal layers imaged by optical coherence tomography. Am J Ophthalmol 2005;139:1056-61.
11. Unterhuber A, Hermann B, Sattmann H, Sattmann H, Drexler W, Yakovlev V, et al. Compact, low cost Ti:Al2O3 laser for in vivo ultrahigh resolution optical coherence tomography. Opt Lett 2003;28:905-7.
12. Gloesmann M, Hermann B, Schubert C, Sattmann H, Ahnelt PK, Drexler W. Histologic correlation of pig retina radial stratification with ultrahigh-resolution optical coherence tomography. Invest Ophthalmol Vis Sci 2003;44:1696-703.
13. Anger EM, Unterhuber A, Hermann B, Sattmann H, Schubert C, Morgan JE, et al. Ultrahigh resolution optical coherence tomography of the monkey fovea. Identification of retinal sublayers by correlation with semithin histology sections. Exp Eye Res 2004;78:1117-25.
14. Lim JI, Tan O, Fawzi AA, Hopkins JJ, Gil-Flamer JH, Huang D. A pilot study of fourier-domain optical coherence tomography of retinal dystrophy patients. Am J Ophthalmol 2008;146:417-26.
15. Early Treatment Diabetic Retinopathy Study Research Group. ETDRS report number 10: grading diabetic retinopathy from stereoscopic color fundus photographs-an extension of the modified Airlie House classification. Ophthalmology 1991;98:786-806.
16. Wolsley CJ, Saunders KJ, Silvestri G, Anderson RS. Investigation of changes in the myopic retina using multifocal electroretinograms, optical coherence tomography and peripheral resolution acuity. Vision Res 2008;48:1554-61.
17. Aleman TS, Cideciyan AV, Sumaroka A, Schwartz SB, Roman AJ, Windsor EA, et al. Inner retinal abnormalities in X-linked retinitis pigmentosa with RPGR mutations. Invest Ophthalmol Vis Sci 2007;48:4759-65.
18. Ito Y, Nakamura M, Yamakoshi T, Lin J, Yatsuya H, Terasaki H. Reduction of inner retinal thickness in patients with autosomal dominant optic atrophy associated with OPA1 mutations. Invest Ophthalmol Vis Sci 2007;48:4079-86.
19. Matsumoto H, Kishi S, Otani T, Sato T. Elongation of photoreceptor outer segment in central serous chorioretinopathy. Am J Ophthalmol 2008;145:162-8.
20. Falkenberry SM, Ip MS, Blodi BA, Gunther JB. Optical coherence

tomography findings in central retinal artery occlusion. Ophthalmic Surg Lasers Imaging 2006;37:502-5.

21. Sivaprasad S, Ikeji F, Xing W, Lightman S. Tomographic assessment of therapeutic response to uveitic macular oedema. Clin Expt Ophthalmol 2007;35:719-23.
22. Bagci AM, Shahidi M, Ansari R, Blair M, Blair NP, Zelkha R. Thickness profiles of retinal layers by optical coherence tomography image segmentation. Am J Ophthalmol 2008;146:679-87.
23. Tan O, Li G, Lu AT, Varma R, Huang D, Advanced Imaging for Glaucoma Study Group. Mapping of macular substructures with optical coherence tomography for glaucoma diagnosis. Ophthalmology 2008;115:949-56.
24. Chan A, Duker JS, Ishikawa H, Ko TH, Schuman JS, Fujimoto JG. Quantification of photoreceptor layer thickness in normal eyes using optical coherence tomography. Retina 2006;26:655-60.
25. Baroni M, Fortunato P, La Torre A. Towards quantitative analysis of retinal features in optical coherence tomography. Med Eng Phys 2007;29:432-41.
26. Sadda SR, Joeres S, Wu Z, Updike P, Romano P, Collins AT, et al. Error correction and quantitative subanalysis of optical coherence tomography data using computer-assisted grading. Invest Ophthalmol Vis Sci 2007;48:839-48.